Preparation and Characterization of Metal Nanoparticles on a Diamond Surface

Jin-Song Gao, Tiruchirapalli Arunagiri, Jin-Jian Chen, Patrick Goodwill, and Oliver Chyan*

Department of Chemistry, University of North Texas, Denton, Texas 76203

Jose Perez and David Golden

Department of Physics, University of North Texas, Denton, Texas 76203

Received June 6, 2000. Revised Manuscript Received September 5, 2000

The deposition of metal nanoparticles (such as Ag, Cu, Au, Pd, and Pt) on boron-doped, polycrystalline diamond thin films grown on silicon substrates was investigated using Raman spectroscopy, scanning electron microscopy, X-ray photoelectron spectroscopy, and X-ray diffraction. Nanometer-size metal particles with preferred crystalline textures can be spontaneously deposited on the diamond thin film after a simple immersion in an acidic solution containing metal ions or metal complex ions. The size and distribution of metal deposits can be controlled by adjusting the metal ions concentration, the solution acidity, and the deposition time. The diamond/silicon interfacial ohmic contact was found to be the critical factor for achieving the observed spontaneous metal deposition on the diamond surface. Significant enhancement of hydrogen evolution activity was observed on a diamond electrode modified by 9% coverage of Pd nanoparticles. The results demonstrate a novel route for depositing nanometer-size metal catalysts on a highly corrosion resistant and dimensionally stable polycrystalline diamond support.

Introduction

The growth of diamond thin films on metal and nonmetal substrates by chemical vapor deposition (CVD) has been well-established. The synthetic diamond thin films possess several technologically important properties: high thermal conductivity, hardness, adjustable conductivity via doping, optical transparency, corrosion resistance/chemical inertness, and the ability to pattern the electrode geometry using selective growth techniques.[1] Potential applications to take advantage of these useful properties in high-power electronic devices, field emission flat panel displays, coatings for cutting tools, and electrooptical devices have been proposed.[1b] Recently, there is a growing interest in investigating the electrochemical and spectroscopic characteristics of solid/liquid interfaces formed on conductive and semiconductive boron-doped diamond thin films.[2−5] In the area of metal deposition on boron-doped diamond, Swain et al. have studied the electrochemical deposition of Pt, Pb, and Hg adlayers on conductive diamond thin-film surfaces and demonstrated that the Hg-coated diamond electrode can be used in the determination of Pb^{2+} and Cu^{2+} using anodic stripping voltammetry.[2d] Most recently, incorporation of noble metals in boron-doped diamond during synthesis to enhance the catalytic properties has been demonstrated.[4] Also, lithium metal deposition on single-crystal and polycrystalline diamond electrodes from a solid polymer electrolyte in ultrahigh vacuum has been presented.[5] Most recently, Miller et al. reported a mechanistic study of silver and mercury electrochemical deposition on boron-doped diamond and found that the nucleation depends on overpotential and metal ion concentration.[6]

This paper presents a novel method for the deposition of metal nanoparticles on boron-doped, polycrystalline diamond thin films grown on p-type silicon substrates. By a simple solution immersion, nanoparticles of such metals as silver, copper, gold, palladium, and platinum

* Corresponding author. Tel: (940) 565-3463. E-mail: Chyan@unt.edu.

(1) Spear K. E.; Dismukes E. J. P., Eds. *Synthetic diamond: Emerging CVD Science and Technology*; John Wiley and Sons: New York, 1994. (b) Pan, L. S.; Kania, D. R., Eds. *Diamond: Electronic Properties and Applications*; Kluwer Academic Publishers: Boston, 1995. (c) Angus, J. C.; Hayman, C. C. *Science* **1988**, *241*, 913. (d) Geis, M. W.; Angus, J. C. *Sci. Am.* **1992**, *267*, 84. (e) Davis, R. F. *J. Cryst. Growth* **1994**, *137*, 161. (f) Werner M.; Locher, R. *Rep. Prog. Phys.* **1998**, *61*, 1665.

(2) Swain, G. M.; Ramesham, R. *Anal. Chem.* **1993**, *65*, 345. (b) Swain, G. M. *J. Electrochem. Soc.* **1994**, *141*, 3382. (c) Awada, M.; Strojek, J. W.; Swain, G. M. *J. Electrochem. Soc.* **1995**, *142*, L42. (d) Alehashem, S.; Chambers, F.; Strojek, J. W.; Swain, G. M. *Anal. Chem.* **1995**, *67*, 2812.

(3) Pleskov, Y. V.; Sakharova, Y.; Krotova, M. D.; Bouilov, L. L.; Spitsyn, B. V. *J. Electroanal. Chem.* **1987**, *228*, 19. (b) Yano, T.; Tryk, A.; Fujishima, A. *J. Electrochem. Soc.* **1998**, *145*, 1870. (c) Martin, H. B.; Argoitia, A.; Angus, J. C.; Landau, U. *J. Electrochem. Soc.* **1999**, *146*, 2959. (d) Zhu, P. L.; Zhu, J. Z.; Yang, S. Z.; Zhang, X. K.; Zhang, G. X. *Fresenius J. Anal. Chem.* **1995**, *353*, 171.

(4) Wang, J.; Swain, G. M.; Tachibana, T.; Kobashi, K. *Electrochem. Solid State Lett.* **2000**, *3*, 286. (b) Pleskov, Y. V. *Russ. Chem. Rev. (Engl. Transl.)* **1999**, *68*, 381. (c) Evstefeeva, Y. E.; Khanova, L. A.; Pleskov, Y. V.; Baranov, A. M. *Russ. J. Electrochem.* **1999**, *35*, 1125.

(5) Li, L. F.; Totir, D.; Miller, B.; Chottiner, G.; Argoitia, A.; Angus, J. C.; Scherson, D. A. *J. Am. Chem. Soc.* **1997**, *119*, 7875. (b) Li, L. F.; Totir, D.; Vinokur, N.; Miller, B.; Chottiner, G.; Evans, E. A.; Angus, J. C.; Scherson, D. A. *J. Electrochem. Soc.* **1998**, *145*, L85.

(6) Vinokur, N.; Miller, B.; Avyigal, Y.; Kalish, R. *J. Electrochem. Soc.* **1999**, *146*, 125.

10.1021/cm000465o CCC: $19.00
Published on Web 11/02/2000

can be spontaneously deposited on the diamond thin film. The metal nanoparticles were characterized by scanning electron microscopy and X-ray photoelectron spectroscopy. The crystalline features of the metal nanoparticles were determined using X-ray diffraction measurement. No preferential deposition on the intercrystalline grain boundaries was observed; instead, the metal nanoparticles were distributed evenly over the diamond microcrystal facets. The size of metal nanoparticles and their distribution can be controlled by the concentration of metal ions, the solution acidity, and the deposition time. Our data show that the silicon substrate functions as an internal electron source to afford spontaneous metal deposition on the boron-doped diamond surface. The new deposition route could significantly simplify the preparation of new metal/diamond, which combines the excellent corrosion resistance and dimensional stability of polycrystalline diamond films with the catalytic activity of metal nanoparticles.

Experimental Section

Polycrystalline diamond films (ATM Inc.) were grown on Si(100) (p-type, 0.01 Ω cm) substrates in a hot-tungsten filament assisted chemical vapor deposition system following previously reported growth conditions.[7] Si(100) substrates were dipped in a 1:1 H_2O:HF, dried with a stream of N_2 and seeded with diamond-powder suspension to enhance the nucleation density. Boron doping was achieved by adding diborane (2000 ppm in UHP H_2) to the source gas. To remove residual graphite and to ensure hydrogen termination, the as-grown diamond sample was placed under continued hydrogen flow with the filament at the growth temperature for 30 min after source gases were stopped. The thickness of the diamond film was ca. 65 μm (growth time = 472 h.) based on the cross sectional SEM imaging. Free-standing diamond film could be peeled off from its silicon back support. The silicon residue on the diamond film was removed by silicon etching solution (HNO_3/CH_3COOH/HF, 67:25:8). The average conductivity of the free-standing diamond film was measured by a four-point probe to be 0.12 Ω^{-1} cm^{-1}.

The diamond/silicon wafer was first cut into 1 cm × 1 cm chips. Prior to metal deposition, the chip was immersed in a cleaning solution (NH_4OH/H_2O_2/H_2O, 1:1:5) for 10 min and then in hydrofluoric acid (4.9%, electronic grade) for 10 min, followed by an ultrapure water rinse. The metal deposition solutions were prepared by diluting corresponding ICP metal standard solutions (Aldrich) with ultrapure hydrofluoric acid of three different strengths (0.0049%, 0.049%, 0.49%). The metal deposition was performed by leaving the diamond/silicon chip undisturbed at the bottom of the PFA (perfluoroalkoxy polymer) beaker containing the solution, for a certain period of time. Thus the immersion exposed both the diamond surface and its silicon back substrate to the deposition solution. The sample was then rinsed thoroughly with ultrapure water and dried by a stream of N_2 before surface characterization. All PFA labwares were carefully cleaned to avoid contamination.[8]

A SPEX 1403 double monochromator equipped with a photomultiplier was used for Raman measurements. The excitation line was 514.5 nm from a Coherent Model Innova 90 argon ion laser. Scanning electron microscopy (SEM) was performed with a JEOL JSM-T300 electron microscope. The X-ray photoelectron spectroscopy (XPS) studies were conducted with an ESCALAB MKII spectrometer (VG Scientific Ltd.). Al K_α X-ray was used as the excitation source for the XPS measurement. X-ray diffraction (XRD) patterns were run on a Siemens D500 diffractometer using Cu K_α radiation. The tube source was operated at 40 kV and 30 mA. Two theta (2θ) scans were performed using a curved graphite monochromator with 0.05° and 1° slits mounted on the source and two 1° slits mounted before a scintillation detector. Scans were run at 0.05° per step and 1 s dwell time. Data were collected using MDI Datascan 3.2 software with a DACO interface.

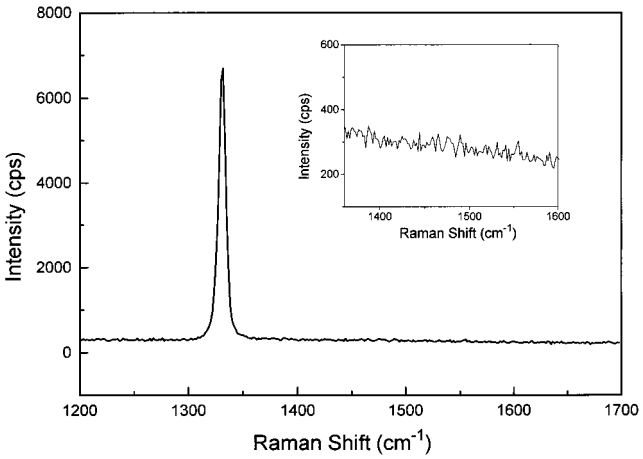

Figure 1. Raman spectrum of the boron-doped polycrystalline diamond thin film.

The electrochemical measurements were performed using an EG&G 273 potentiostat in a standard three-electrode cell with a platinum counter electrode and Ag/AgCl (3M KCl) reference electrode. Ar gas was bubbled through the solution in order to remove air oxygen. Both diamond and diamond/silicon free-standing films were used as the working electrodes. The electrical contact to diamond film was made by silver epoxy to copper wire. The electrode was insulated, except for the front diamond surface using a silicone rubber (GE, 100% silicone). The diamond electrode was cleaned in (NH_4OH/H_2O_2/H_2O, 1:1:5) for 30 min prior to each run to remove metal deposition and subsequently rinsed thoroughly with ultrapure water.

Results

Figure 1 shows the Raman spectrum of a boron-doped, polycrystalline diamond thin film grown on silicon substrate used in this study. An intense and sharp Raman line originating from the bulk diamond sp^3 structure appears at 1332 cm^{-1} with a full width at half-maximum (fwhm) of 7 cm^{-1}. The Raman excitation is assigned on the basis of the literature to the triply degenerate optical phonon F_{2g} belonging to space group O_h.[9] No discernible peak was observed at ~1500 cm^{-1} (see the inset of Figure 1), indicating the high quality of the diamond film, with no detectable sp^2 carbon impurities.

In Figure 2a, the SEM image reveals that the diamond thin film is composed of well-faceted randomly oriented microcrystallites of approximately 10−20 μm. After immersion in 1 ppm Ag^+/HF solutions, nonaggregating submicron (ca. 50−400 nm) particles were found to deposit evenly over the polycrystalline diamond surfaces (cf. Figure 2b−d). It is important to note that the nanoparticles formation took place spontaneously after a simple solution immersion. The chemical com-

(7) Miller, J. B.; Brandes, G. R. *J. Appl. Phys.* **1997**, 82, 4538. (b) Brandes, G. R.; Beetz, C. P.; Feger, C. F.; Wright, R. W.; Davidson, J. L. *Diamond Relat. Mater.* **1999**, *8*, 1936.

(8) Chyan, O.; Chen, J. J.; Chen, L.; Xu, F. *J. Electrochem. Soc.* **1997**, *144*, L17. (b) Chyan, O.; Chen, J. J.; Xu, F.; Sees, J.; Hall, L. *Analyst* **2000**, *125*, 175.

(9) Ishida H., Ishitani, A. *Appl. Spectrosc.* **1983**, *37*, 450, (b) Solin, S. A.; Ramdas, A. K. *Phys. Rev. B* **1970**, *1*, 1687.

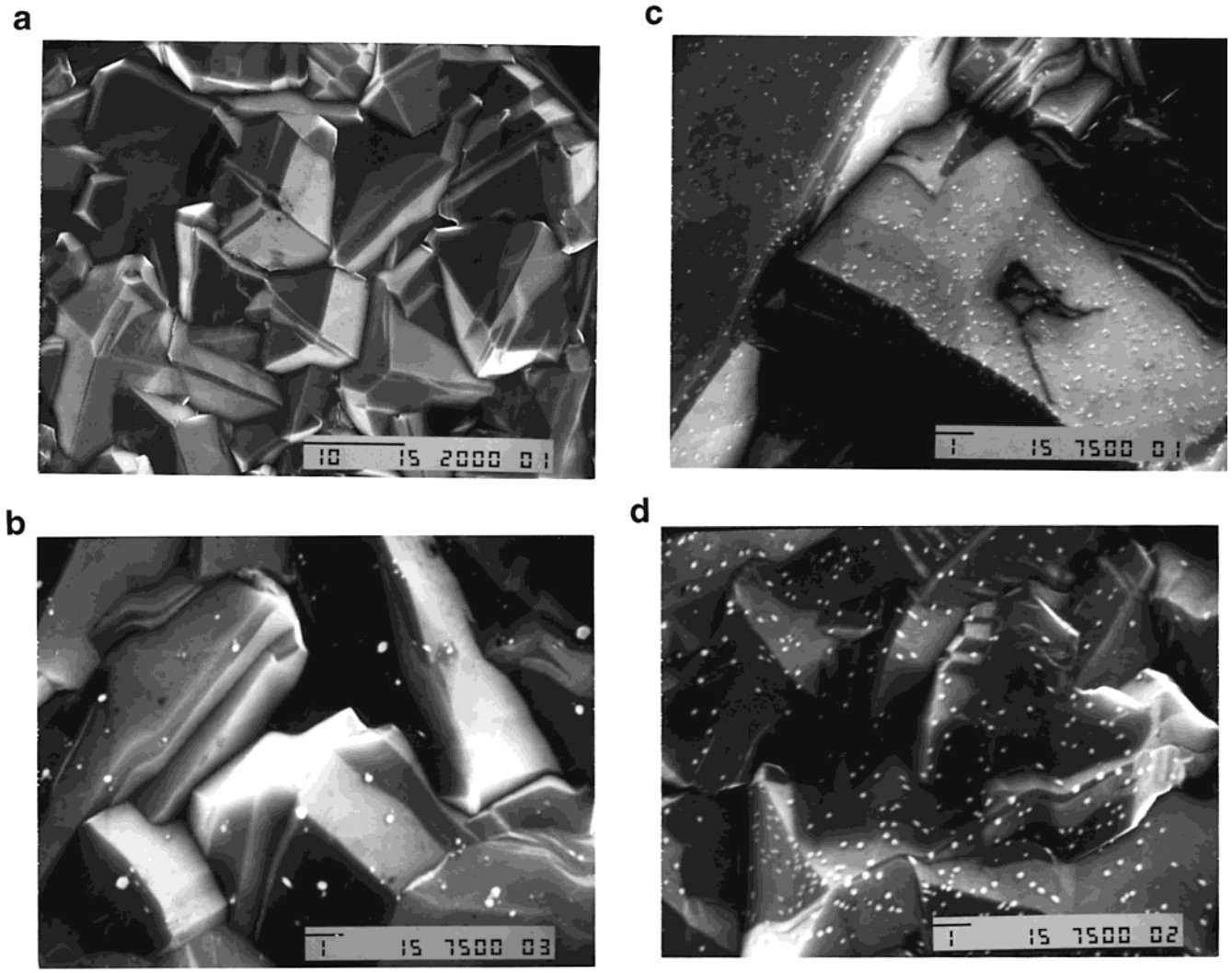

Figure 2. SEM images of diamond thin films before (a) and after (b−d) Ag deposition. The deposition solution is (b) 1 ppm Ag^+/0.0049% HF, (c) 1 ppm Ag^+/0.049% HF, and (d) 1 ppm Ag^+/0.49% HF, respectively. The deposition time is 2 h.

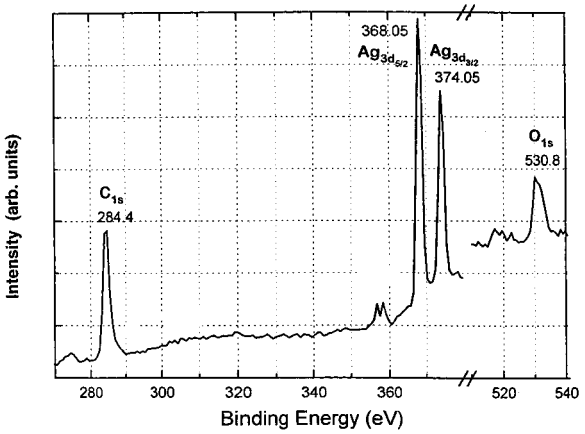

Figure 3. XPS spectrum of the boron-doped polycrystalline diamond thin film covered by the Ag nanoparticles.

position of nanoparticles was analyzed by X-ray photoelectron spectroscopy (XPS). Figure 3 shows two strong XPS peaks that were observed in addition to C_{1s} and O_{1s} peaks resulting from the diamond substrate and background. Both the binding energies (368.05 and 374.05 eV) and intensity ratio of the two dominant XPS peaks correspond well with the Ag $3d_{5/2}$ and $3d_{3/2}$ lines for elemental Ag.[10] In addition, the peak intensity was found to increase with the deposition coverage of nanoparticles. Other minor XPS peaks also support that the nanoparticles on diamond surface were predominantly Ag.

In Figure 4, XRD patterns reveal that crystalline phases exist in the Ag nanoparticles formed on the diamond surface by solution immersion. By comparing to the diamond substrate background (see the insert of Figure 4), the XRD data indicate preferred textures on Ag nanoparticle growth along ⟨220⟩ and to a lesser extent along ⟨111⟩ crystallographic orientation. Both XPS and XRD data support that the nanoparticles deposited on diamond are mostly zero-valence silver metal with crystalline phases of preferred orientations. In a series of follow-up experiments, we also observed the spontaneous deposition of Au, Cu, Pd, and Pt metal particles on the diamond thin film grown on silicon substrate by a simple immersion in solutions of corresponding metal ions.

The solution chemistry can affect the particle size and deposition coverage of Ag nanoparticles formed on the diamond surface by solution immersion. Figure 2b−d

(10) Wagner, C. D.; Riggs, W. M.; Davis, L. E.; Moulder, J. E.; Mulienberg, G. E.; Eds. *Handbook of X-ray photoelectron spectroscopy*. Perkin-Elmer Corp.: Eden Prairie, p 112.

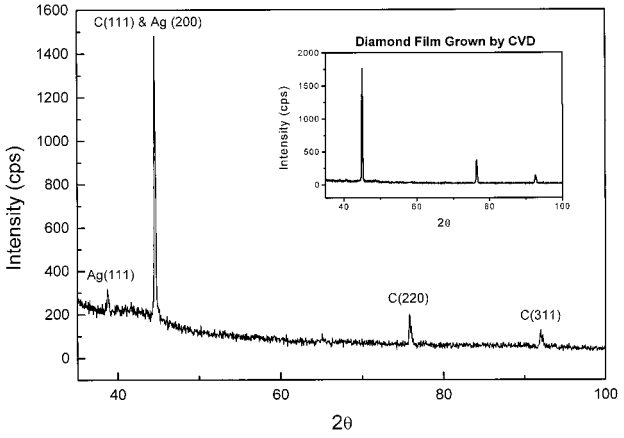

Figure 4. XRD of the boron-doped polycrystalline diamond thin film covered by Ag nanoparticles.

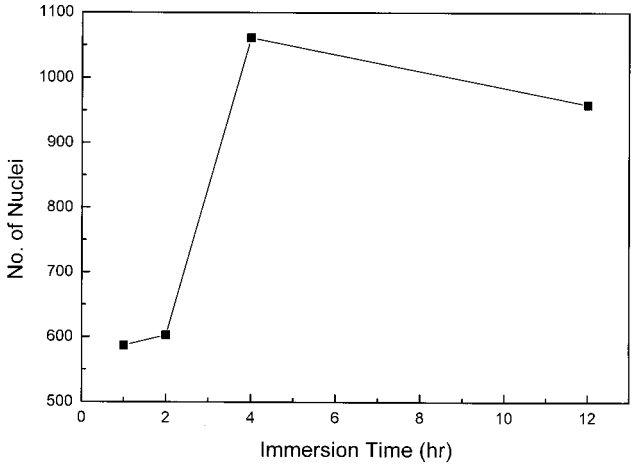

Figure 5. Time-dependent study of the nucleation of Ag on a diamond surface. The solution is 1 ppm Ag^+/0.49% HF.

illustrates the observed relationship between the size of the Ag particles and the HF concentration. When the diamond sample was immersed in a solution of 0.49% HF/1 ppm Ag^+ for 2 h, the size of the silver deposits has a range of ca. 100−250 nm. In the more dilute 0.049% HF/1 ppm Ag^+, a smaller but denser silver deposit with particle diameter of 50−130 nm was observed. However, much less nucleation and significantly larger silver particles (50−400 nm) were found on diamond surface in the most dilute 0.0049% HF/1 ppm Ag^+. It is interesting to note that the number of Ag particles deposited on the diamond surface is roughly inversely proportional to the size of the Ag nanoparticles. A similar trend of particles size and distribution was also observed for the Pd, Cu, Pt, and Au nanoparticles.

We further investigated the effect of metal ion concentration and deposition time on the nucleation and growth of metal nanoparticles on the diamond surface. The diamond/silicon sample was immersed in 1 ppm Ag^+/0.49% HF solution with incremental deposition times of 1, 2, 4, and 12 h. At the end of each deposition period, the diamond sample was removed and observed under SEM after it was rinsed with ultrapure water and dried by N_2. Our SEM experimental setup allows the same location (ca. 30 μm × 24 μm) to be repeatedly examined after each immersion period. The deposition of Ag on the diamond surface in 1 ppm Ag^+/0.49% HF was found to be via a progressive nucleation process. Figure 5 shows that the number of silver nuclei increases with time to reach a plateau and decreases slightly at the end of 12 h. The decrease could be partially caused by some coalescence of adjacent Ag nuclei observed by SEM at the end of 12 h. In contrast, the Ag nucleation on the diamond surface was found to be more instantaneous in the more concentrated 100 ppm Ag^+/0.49% HF solution. With a higher Ag^+ ion concentration, the maximum nucleation was reached within 60 s of immersion. In addition, extensive coalescence of Ag nuclei and dendritic Ag growth were clearly seen on the diamond surface after an additional 30 min of immersion. In both cases, SEM images showed that Ag deposits were evenly distributed over the diamond crystalline facets with no preferred deposition on intercrystalline grain boundaries.

Discussion

To spontaneously deposit metal particles on a diamond surface, excess electrons must be made available to reduce the metal ions near the solution/diamond interface. In this study, the electron sources were generated and maintained from within the chemical system, since no external electron source was used. The surface defects such as nondiamond sp^2 carbon defects could potentially serve as an additional electron source on the diamond surface to afford spontaneous metal deposition.[11] However, our Raman data indicate that there is no detectable nondiamond sp^2 carbon impurities on the diamond film both prior to and after the metal deposition. Furthermore, no preferential Ag deposit on the intercrystalline grain boundary, where the nondiamond sp^2 carbon surface defects are most likely located, was observed. Instead, Ag particles were found to deposit uniformly over the various facets of the diamond crystallites (Figure 2b−d).

To further investigate the metal deposition mechanism, we isolated the diamond film from its silicon substrate. A 65 μm free-standing diamond film was peeled off from its silicon back support. The silicon residue on the diamond film was completely removed with silicon etching solution. Then, the diamond film was immersed in a solution of 100 ppm Ag^+/0.49% HF together with another control diamond/silicon sample. No silver deposits were observed on the free-standing diamond film while the control diamond/silicon sample was again covered uniformly with a layer of silver deposits. In addition, one can resume the spontaneous Ag particle deposition on the diamond surface by simply placing the free-standing diamond film in contact with a silicon chip immersed in the Ag^+-containing HF solution. Our experimental results demonstrated that the electrons responsible for the observed spontaneous metal deposition did not originate from the diamond film but from the underlying silicon substrate.

Previous reports[12] including our atomic force microscopic data[13] have demonstrated that metal nanoparticles (including Cu, Ag, Pt, Pd, and Au) can be readily deposited on the hydrogen-terminated silicon surface

(11) DeClements R.; Swain, G. M. *J. Electrochem. Soc.* **1997**, *144*, 856.

when placed in contact with the metal ion containing solutions. Driven by the simultaneous oxidative etching of the silicon surface, the metal deposition process is highly thermodynamically favorable. This displacement deposition mechanism was further supported by the AFM data, which showed extensive surface roughening and nanoscale pit formation caused by the metal-deposition-induced silicon surface corrosion. However, no metal deposits can be observed on the silicon surfaces covered with a thin surface oxide. The potentiometric data[13b] revealed that the open-circuit potential of the hydrogen-terminated silicon surface is more than 700 mV negative than the oxide-covered silicon surface. This observation suggests that the hydrogen-terminated silicon surface is more reductive (i.e., electron rich) than its oxide-covered counterpart. Therefore, the more reductive hydrogen-terminated silicon surface can effectively attract and reduce metal ions from solution to form the corresponding metal nanoparticles. SEM images of silicon substrate on which the diamond film was grown indeed showed extensive metal deposition after immersion in Ag^+/HF solution.

In contrast, our present study indicates that the free-standing hydrogen-terminated diamond surface alone is not capable of reducing Ag^+ ions. The observation is consistent with the well-known excellent chemical stability of diamond. Furthermore, no metal deposition-induced surface roughening and pit formation were found on diamond surfaces (Figure 2b−d), further indicating that the diamond film is not directly responsible for the observed metal deposition. We propose that the surface electron energy of the conductive diamond film is raised significantly through the direct electrical contact with the underlying more reductive hydrogen-terminated silicon substrate. The excess electrons, originating from the silicon/HF solution interface due to oxidation of silicon, migrate to the diamond surface to achieve the observed spontaneous metal deposition. This assertion corroborates well with the activation of the Ag deposition process on the diamond surface by simply placing the free-standing diamond film in contact with a silicon chip immersed in Ag^+-containing HF solution.

The early stage of Ag electrocrystallization on metal or carbon electrode surfaces has been well-studied and shown to be strongly dependent on the overpotential.[14] Barton and Bockris studied the growth of individual dendrites of Ag from the tip of Ag microelectrode and proposed that the origin of the dendrites lies in the prismatic growths at the early state of electrocrystallization.[15] Despic and Purenovic showed a critical overpotential threshold for initiating dendritic growth.[15] Most recently, Vinokur et al. applied a potentiostatic current transient technique to demonstrate the influence of overpotential and concentration on the Ag nucleation on a boron-doped diamond surface.[6] In this study, exact assessment of the overpotential to the Ag nucleation is not feasible, since the electrochemical potential is generated internally from the silicon/solution interface. However, some semiquantitative interpretation can be made on the basis of the electrochemistry of Ag^+ ion on the silicon substrate surface. The electrochemical driving force, i.e., overpotential, for Ag nucleation on diamond is mainly controlled by the difference of the Ag^+ reduction potential and silicon oxidation potential. With a 100-fold increase of the Ag^+ ion concentration, the reduction of Ag^+ will be more thermodynamically favorable on the basis of the Nernst equation. The resulting higher overpotential drives the Ag deposition on diamond surface from progressive nucleation toward more instantaneous nucleation. The observed extensive coalescence of Ag nuclei and dendritic Ag growth on the diamond surface in 100 ppm Ag^+/0.49% HF solution corresponds well with the Ag electronucleation morphology commonly seen in the higher overpotential condition.

However, the effect of HF concentration on the Ag nucleation process on a diamond surface is more complex. The increase of HF concentration enhances the solution acidity, which directly affects the electrochemical potential of the silicon substrate. To assess the effect, we measured the open circuit potential of silicon substrate immersed in HF solutions. The silicon potentials were found to be −240, −290, and −327 mV vs Ag/AgCl in 0.0049%, 0.049%, and 0.49% HF, respectively. Therefore, the higher HF strength will make the silicon surface more reductive at the silicon/HF interface. Consequently, the Ag deposition process will be more thermodynamically favorable, i.e., higher overpotential, in 0.49% HF vs 0.0049% HF solution. The observed Ag nucleation morphologies in Figure 2b−d seem to partially support the above assertion. For example, the more densely deposited Ag nuclei with rather uniform particle size distribution in Figure 2d suggest that the instantaneous Ag nucleation is more likely to be favorable in 0.49% HF/Ag^+ solution. However, the actual Ag deposition on the silicon surface involves a rather complex surface corrosion process. The reductive, hydrogen-terminated silicon surface is maintained by HF, which etches away oxidized silicon caused by the Ag deposition. In HF solution, there are three chemical equilibria in operation to generate chemical species including HF, F^-, HF_2^-, $(HF)_2$, and H^+, which have very different etching kinetics and characteristics. For instance, metal-deposition-induced surface roughening and pit formation tend to be accelerated on the silicon surface at higher HF concentrations. Therefore, the silicon potential increase caused by higher HF strength is important but is not the only factor controlling the Ag nucleation on the diamond/silicon surface.

In summary, the results demonstrate a novel preparation route for depositing nanometer-size metal particles on a polycrystalline diamond surface grown on a silicon support. The deposition morphology and metal nanoparticle distribution on the diamond surface can be controlled by judicious adjustment of HF concentration and metal ion concentration. The new deposition

(12) Ohmi, T.; Imaoka, T.; Sugiyama, I.; Kesuka, T.; *J. Electrochem. Soc.* **1992**, *139*, 3317. (b) Kniffin, M. L.; Beerling, T. E.; Helms, C. R.; *J. Electrochem. Soc.* **1992**, *139*, 1195. (c) Nagahara, L. A.; Ohmori, T.; Hashimoto, K.; Fujishima, A. *J. Vac. Sci. Technol.* **1993**, *A11(4)*, 763. (d) Nagahara, L. A.; Ohmori, T.; Hashimoto, K.; Fujishima, A. *J. Electroanal. Chem.* **1992**, *333*, 363.

(13) Chyan, O.; Chen, J. J.; Chien, H. Y.; Sees, J.; Hall, L. *J. Electrochem Soc.* **1996**, *143*, 92. (b) Chyan, O.; Chen, J. J.; Chien, H. Y.; Wu, J. J.; Liu, M.; Sees, J.; Hall, L. *J. Electrochem. Soc.* **1996**, *143*, L235.

(14) Kaischew, B.; Mutaftchiew, B. *Electrochim. Acta* **1965**, *10*, 643. (b) Fleischmann, M.; Thirsk, H. R. *Electrochim. Acta* **1960**, *2*, 22. (c) Astley, D. J.; Harrison, J. A.; Thirsk, H. R. *Trans. Faraday Soc.* **1968**, *64*, 172. (d) Scharifker, B.; Hills, G. *Electrochim. Acta* **1983**, *28*, 879.

(15) Barton, J. L.; Bockris, J. O'M. *Proc. R. Soc.* **1962**, *A268*, 485.

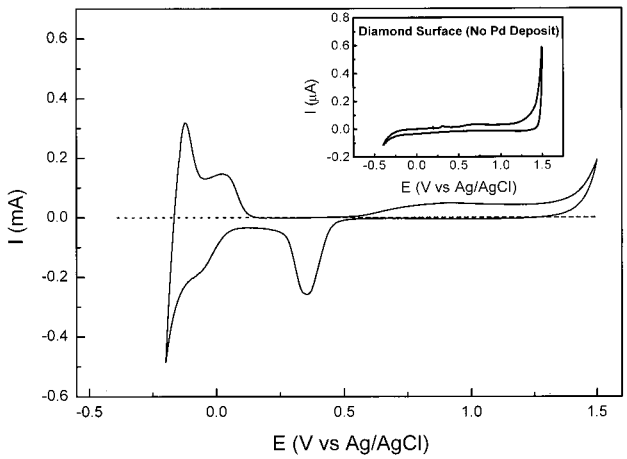

Figure 6. Solid curve: cyclic voltammogram of a diamond electrode modified by ca. 9% coverage of Pd metal nanoparticles in 0.5 M H_2SO_4. Dashed curve and the inset with expanded current scale: cyclic voltammogram of the corresponding bare diamond electrode in 0.5 M H_2SO_4.

route could significantly simplify the preparation of new metal/diamond catalysts, which combines the excellent corrosion resistance and dimensional stability of polycrystalline diamond films with the catalytic activity of metal nanoparticles. Figure 6 illustrates the significant catalytic effect on the interfacial electron transfer process at the diamond electrode surface after it was modified with roughly 9 % coverage of palladium nanoparticles. As shown in Figure 6, the current density was enhanced approximately 3 orders of magnitude, and the potential onset for hydrogen evolution was moved 400 mV more positive with palladium nanoparticle catalyst. Work is currently in progress in our lab to further explore the catalytic applications of the metal nanoparticle/diamond systems.

Acknowledgment. This work has been supported by a grant from the Robert A. Welch Foundation. We also would like to thank Dr. Chuck Christ for providing initial diamond sample and Dr. Teresa Golden for the XRD measurements.

CM000465O